Sliding friction of multilayer ^{4}He films adsorbed on graphite

Nariko Hosomi and Masaru Suzuki*
Department of Applied Physics and Chemistry, University of Electro-Communications, Chofu, Tokyo 182-8585, Japan
(Received 30 August 2007; published 2 January 2008)

We have carried out a quartz crystal microbalance experiment for multilayer ^{4}He films adsorbed on graphite. We analyzed changes in the resonance frequency and Q value using the multilayer model, and obtained the sliding friction of the boundary between the atomic layers in the film, in addition to the boundary between the film and the substrate. The sliding friction of the boundary of the first and second atomic layers is much smaller than that of the boundary between the film and the substrate.

DOI: 10.1103/PhysRevB.77.024501 PACS number(s): 67.25.bh, 68.35.Af, 68.60.−p

I. INTRODUCTION

Slip of an atomic thick film is a particularly important aspect of the sliding friction on a nanometer scale.[1] Krim and co-workers found that several physisorbed films adsorbed on metal substrates undergo slipping relative to the oscillating substrate.[2,3] Mistura and co-workers also observed the slip of films under certain conditions.[4,5] In fluid mechanics, the slip of shear flow past a solid surface is also a fundamental problem that has long been an object of discussion. One of the simplest boundary conditions is the no-slip condition, for which the relative velocity of fluid adjacent to the surface is zero. However, experimental evidence of slip at the surface was recently reported for Newtonian fluids.[6,7]

More recently, Casey *et al.* carried out measurements for the slip of normal ^{3}He thin slabs, and investigated the intermediate region between the two limiting cases of flow of bulk liquid past a planar surface and slip of an atomic monolayer film adsorbed on a substrate.[8] They interpreted their data in terms of an interfacial friction model, i.e., a ^{3}He slab as a rigid object is coupled by a frictional force to the oscillating substrate. However, from a microscopic point of view, it is not clear where the slip occurs with a frictional force. It is therefore of great interest to determine which boundary slips in the case of multilayer films, the boundary between the film and the substrate or that between the atomic layers in the film. It is well known that noble gases adsorbed on graphite grow in layers. We have carried out a quartz crystal microbalance (QCM) experiment for multilayer ^{4}He films adsorbed on Grafoil (exfoliated graphite), and determined the sliding friction of the boundary between the atomic layers in the film, in addition to the boundary between the film and the substrate.

In the QCM experiment for *monolayer* film, the sliding friction is obtained from the changes in the resonance frequency and Q value of the quartz crystal.[9,10] When the friction is proportional to the sliding velocity v as $F=-(\sigma/\tau)\cdot v$, where σ is the areal mass density of the film, these changes are related to the slip time τ as

$$\frac{\Delta f_R}{f_R} = -\frac{\sigma}{M}\frac{1}{1+(\omega\tau)^2}, \tag{1}$$

$$\Delta\left(\frac{1}{Q}\right) = \frac{2\sigma}{M}\frac{\omega\tau}{1+(\omega\tau)^2}, \tag{2}$$

where M is the areal mass density of the crystal and ω is the angular frequency of oscillation. τ can be calculated without requiring the areal mass density of the film.

However, these equations are limited to monolayer film. If the film is multilayer and the slip occurs at the boundary between the atomic layers in the film, they must be modified. In Sec. III, we explain the relation between the changes in the resonance frequency and Q value and the sliding friction of each boundary. In the multilayer model, the slip between the atomic layers in the film is allowed. In Sec. IV, we describe our experimental results of multilayer ^{4}He films adsorbed on Grafoil. Then, in Sec. V, we analyze these results and explain the sliding friction of the films.

II. EXPERIMENTAL PROCEDURE

The experimental procedure has been reported in detail elsewhere;[11] here, we describe it briefly. In our experiments, the resonator is a 5.0 MHz AT-cut quartz crystal. Grafoil was first baked in 5×10^{-5} Pa at 900 °C for 3 h, and a 300 Å thick film of Ag was deposited onto it. To bond Grafoil on the Ag electrode, the crystal and Ag-plated Grafoil were pressed together and were heated in 1×10^{-5} Pa at 350 °C for 2 h. After bonding, the excess amount of Grafoil was removed. To retain good thermal contact, the crystal was fixed to the metal holder with electrically conductive adhesive. The Q value of the crystal was better than 10^4. After being heated in 2×10^{-6} Pa at 130 °C for 5 h, the crystal was mounted in the sample cell. During transport, it was briefly (1 min or less) exposed to air. Then, the sample cell was evacuated and cooled down to 4.2 K. To minimize the effect of desorption, Grafoil disks were put on the bottom of the cell.

The graphite crystallites of Grafoil are oriented with their basal planes parallel to the lateral oscillation. The full width at half maximum of the c-axis distribution is 12°, as determined by x-ray scattering. From the specific surface area of 15.4 m^2g, and the change in the resonance frequency from bare Ag to Grafoil/Ag electrodes, the sensitivity for the mass loading of ^{4}He is estimated to be 4.2 Hz/atoms nm^2.[12]

The resonance frequency and Q value were measured using a transmission circuit.[13] In the circuit, the quartz crystal

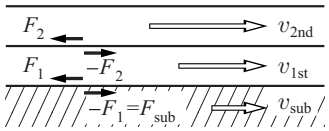

FIG. 1. Bilayer model.

was placed in series with a coaxial line connecting a 50 Ω cw signal generator and a homemade phase-sensitive detector. The frequency of the signal generator was then controlled in order to keep the in-phase signal zero, and was locked to the resonance frequency. The quadrature signal at this frequency is the resonance amplitude, and the change in the Q value is calculated from this amplitude.

III. MULTILAYER MODEL

We consider the QCM experiment for the multilayer film in the case that the slip occurs at the boundary between the atomic layers of the film, in addition to the boundary between the film and substrate. Figure 1 shows the bilayer model as an example. The first atomic layer slides relative to the substrate, and the second atomic layer also slides relative to the first one. At the atomic scale, the sliding friction depends on the sliding velocity. In the model, we assume that the sliding friction is proportional to the sliding velocity,[14] i.e., the friction per unit area acting on the first atomic layer from the substrate is expressed as $F_1=-(\sigma_1/\tau_1)(v_{1st}-v_{sub})$. In the same manner, the friction acting on the second atomic layer from the first one as $F_2=-(\sigma_2/\tau_2)(v_{2nd}-v_{1st})$. Here, v_{1st}, v_{2nd}, and v_{sub} are the velocities of the first and second atomic layers and the substrate, σ_1 and σ_2 are the areal mass densities of the first and second atomic layers, and τ_1 and τ_2 are the slip times, respectively. Then, we obtain the equation of motion with respect to each atomic layer of the bilayer film as

$$\sigma_1 \frac{dv_{1st}}{dt} = -\frac{\sigma_1}{\tau_1}(v_{1st}-v_{sub}) + \frac{\sigma_2}{\tau_2}(v_{2nd}-v_{1st}), \tag{3}$$

$$\sigma_2 \frac{dv_{2nd}}{dt} = -\frac{\sigma_2}{\tau_2}(v_{2nd}-v_{1st}). \tag{4}$$

It should be noted that the reaction of F_2 acts upon the first atomic layer, together with F_1.

In the QCM experiment, the crystal oscillates laterally by the application of an alternating voltage between the electrodes. To calculate the motion on the oscillating substrate, we substitute $v_{sub}=v_{sub,0}\exp(j\omega t)$ into Eq. (3), where $v_{sub,0}$ is the velocity amplitude of the substrate and ω is the angular frequency of oscillation. Then, we can obtain its motion and the sliding friction acting on the substrate F_{sub} which is the reaction of F_1 as

$$F_{sub} = F_{sub,0}\exp(j\omega t), \tag{5}$$

where

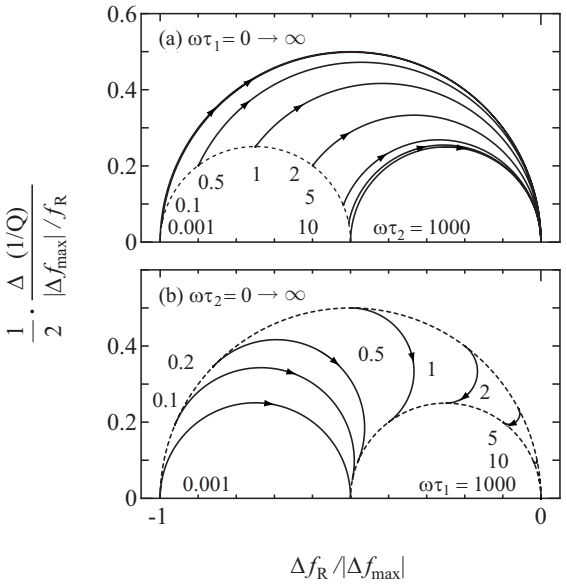

FIG. 2. Dimensionless relationship between $\frac{\Delta f_R}{|\Delta f_{max}|}$ and $\frac{1}{2}\cdot\frac{\Delta(1/Q)}{|\Delta f_{max}|/f_R}$ as a function of $\omega\tau_1$ and $\omega\tau_2$ in the case of $\sigma_1=\sigma_2$. (a) $\omega\tau_1$ varies $0\to\infty$ under the condition when $\omega\tau_2$ is fixed. Each solid line corresponds to a different value of $\omega\tau_2$, and the direction of the arrow indicates the increase of $\omega\tau_1$. (b) $\omega\tau_2$ varies $0\to\infty$ under the condition when $\omega\tau_1$ is fixed.

$$F_{sub,0} = -\frac{\sigma_1}{\tau_1}\frac{j\omega\tau_1 + \frac{\sigma_2}{\sigma_1}\frac{\tau_1}{\tau_2}\frac{j\omega\tau_2}{1+j\omega\tau_2}}{1+j\omega\tau_1 + \frac{\sigma_2}{\sigma_1}\frac{\tau_1}{\tau_2}\frac{j\omega\tau_2}{1+j\omega\tau_2}}v_{sub,0}. \tag{6}$$

Without restricting the bilayer film, we describe F_{sub} in Appendix A.

When an oscillating shearing stress acts upon the surface of the crystal, the resonance frequency and Q value of the crystal change slightly. As shown in Appendix B, the changes in the resonance frequency and Q value are affected by the ratio of $F_{sub,0}$ to $v_{sub,0}$ as

$$\frac{\Delta f_R}{f_R} = -\frac{1}{\omega_R M}\mathrm{Re}\left(\frac{jF_{sub,0}}{v_{sub,0}}\right), \tag{7}$$

$$\Delta\left(\frac{1}{Q}\right) = -\frac{2}{\omega_R M}\mathrm{Im}\left(\frac{jF_{sub,0}}{v_{sub,0}}\right). \tag{8}$$

We examine the changes in the resonance frequency and Q value as a function of $\omega\tau_1$ and $\omega\tau_2$. Here, it is useful to use the dimensionless relationship between $\frac{\Delta f_R}{|\Delta f_{max}|}$ and $\frac{1}{2}\cdot\frac{\Delta(1/Q)}{|\Delta f_{max}|/f_R}$, where Δf_{max} is the mass loading, i.e., the maximum decrease when the film is completely locked to the oscillating substrate at $\omega\tau_1=0$ and $\omega\tau_2=0$.

For example, we illustrate the case of $\sigma_1=\sigma_2$. Figure 2(a) shows the relationship under the condition when $\omega\tau_2$ is fixed and $\omega\tau_1$ varies $0\to\infty$. It draws a semicircle when the second atomic layer is locked to the first one, i.e., $\omega\tau_1$ varies $0\to\infty$ at $\omega\tau_2=0$. Then, the maximum value of $\frac{1}{2}\cdot\frac{\Delta(1/Q)}{|\Delta f_{max}|/f_R}$ is $\frac{1}{2}$

at $\frac{\Delta f_R}{|\Delta f_{\max}|}=\frac{1}{2}$. As $\omega\tau_2$ increases, the semicircle ends halfway and shrinks and $\frac{1}{2}\cdot\frac{\Delta(1/Q)}{|\Delta f_{\max}|/f_R}$ becomes small. Figure 2(b) shows the relationship under the condition when $\omega\tau_1$ is fixed and $\omega\tau_2$ varies $0\rightarrow\infty$. When the first atomic layer is locked to the substrate, i.e., $\omega\tau_1=0$, it draws a small semicircle when $\omega\tau_2$ varies $0\rightarrow\infty$. As $\omega\tau_1$ increases, the position of the semicircle moves. It should be noted that when $\omega\tau_1$ is finite and $\omega\tau_2$ is above a certain value, the resonance frequency *decreases* with *increasing* $\omega\tau_2$, which means that, in contrast to the monolayer film, the increase of $F_{\rm sub}(=-F_1)$ may cause the increase in the resonance frequency. This behavior comes from the phase difference in the oscillating motion between the first and second atomic layers.

Furthermore, it should be noted that in any case of $\omega\tau_1$ and $\omega\tau_2$, the dimensionless relationship is plotted in the region which is surrounded by the semicircles. In the bilayer film, any point in the region corresponds to the only set of $\omega\tau_1$ and $\omega\tau_2$. Using this character, we can determine the set of F_1 and F_2 uniquely from the changes in the resonance frequency and Q value.

Lastly, we comment on the trilayer film. In the same manner, the dimensionless relationship is also plotted in the region surrounded by the semicircles. However, we cannot determine uniquely the set of F_1, F_2, and F_3. Here, F_3 is the sliding friction acting on the third atomic layer from the second one.

IV. EXPERIMENTAL RESULTS

We have carried out the QCM experiment for various ^{4}He areal densities down to 0.35 K. It is well known that ^{4}He film adsorbed on Grafoil grows up to more than five-atom thick film in layers.[15,16] Figure 3 shows the variation of the resonance frequency as a function of temperature. These sets of data were taken during cooling, and the oscillation amplitude of the crystal is about 0.4 nm. The resonance frequency does not greatly change from the empty up to 10 atoms/nm^2, and decreases suddenly at around 11 atoms/nm^2.

As the areal density increases further, it decreases gradually at high temperature with increase in the areal density. At the areal density between 14 and 20 atoms/nm^2, a steplike increase in the resonance frequency is observed below T_S and T_S'. (Here, we define T_S and T_S' as the intersection of the extrapolation from high temperatures and the extension of the steepest increase.) This demonstrates that decoupling of the ^{4}He film from the oscillating substrate occurs below these temperatures. Similar behavior of He films has previously been reported.[17,18] It was found that T_S shifts to lower temperature rapidly around the second layer promotion of 20.4 atoms/nm^2. Above 22 atoms/nm^2, the increase below T_S becomes clear, while the increase below T_S' is smeared out. In addition, T_S appears above the second layer promotion of 12.0 atoms/nm^2. It is concluded that T_S and T_S' are closely related to the layer structure of the ^{4}He film. Decoupling of the ^{4}He film below T_S has been reported elsewhere.[11]

Above 32 atoms/nm^2, decoupling due to superfluidity is observed at T_C, which is in good agreement with torsional oscillator measurements.[16] For the thinner films, we observed no signature of superfluidity.

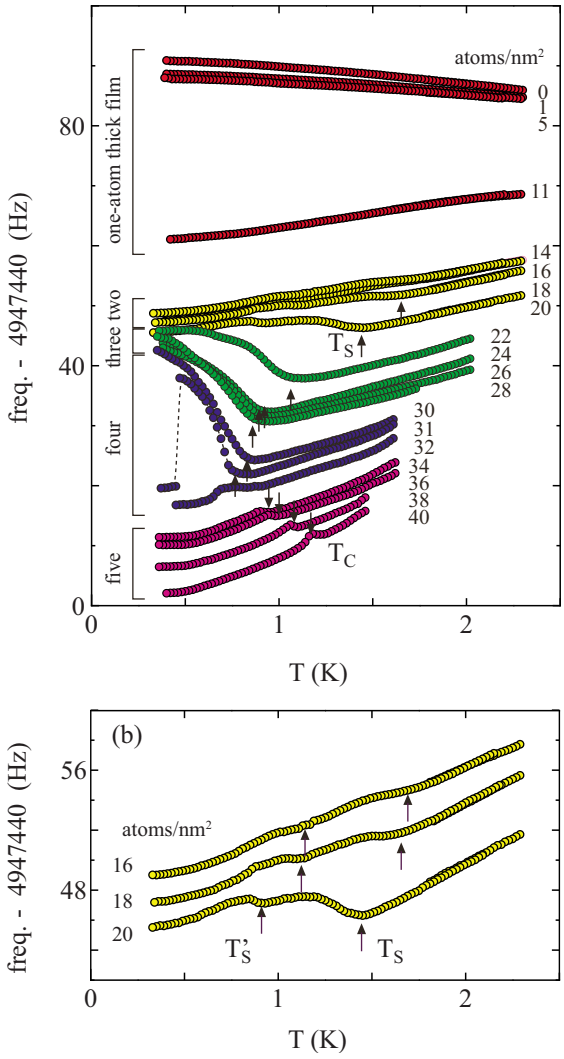

FIG. 3. (Color online) (a) Variation of the resonance frequency for various ^{4}He areal densities as a function of temperature. Different colors correspond to different film thicknesses. (b) Expanded view for the two-atom thick film.

Figure 4 shows the areal density dependence of the changes in the resonance frequency and Q value from the empty at several temperatures. The vertical dotted lines correspond to the layer promotions. The estimated mass loading is represented by the solid line of 4.2 Hz/atoms nm^2 in (a), while the solid one in (b) is the maximum value of $\Delta(1/Q)$, which takes place under the condition that the decrease in resonance frequency is half of the mass loading.

Regardless of temperature, it was found that the decrease in resonance frequency is largely suppressed from the maximum, which means that the film undergoes slipping relative to the oscillating substrate. There also exist some distinct features: (a) The resonance frequency does not change very much in the one-atom thick film, and decreases drastically at around the second layer promotion of 12.0 atoms/nm^2. As the areal density increases further, the frequency decreases gradually but shows some structures. (b) In the three-atom

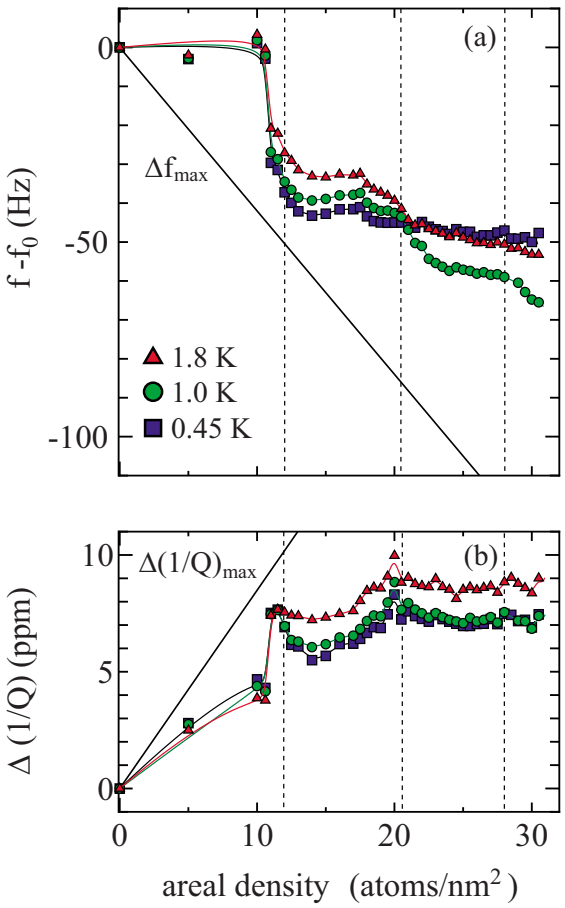

FIG. 4. (Color online) (a) Areal density dependence of the change of the resonance frequency from the empty f_0 at several temperatures. The solid line corresponds to the estimated mass loading of 4.2 Hz/atoms nm^2, which is the possible maximum value. The different colors represent different temperatures. The vertical dotted lines correspond to the layer promotions. (b) Areal density dependence of the change of the Q value from the empty. The solid line is the possible maximum value, which takes place under the condition that the decrease in resonance frequency is half of the maximum decrease.

thick film, the decrease in the resonance frequency at 0.45 K becomes smaller than that of 1.8 and 1.0 K. (c) $\Delta(1/Q)$ shows a small peak slightly below the layer promotions.

V. DISCUSSION

A. Calculation procedure

We analyze the present results using the multilayer model. It is found that the calculation of the monolayer film using Eqs. (1) and (2) cannot be applied to more than the two-atom thick film: Using these equations, both the slip time τ and the areal mass density σ' per unit *the area of electrode* are obtained from the changes in resonance frequency and Q value. Above the two-atom thick film, however, σ' is obviously smaller than the estimated value from the surface area of Grafoil on the electrode.[19]

The discrepancy is caused by a small value of $\Delta(1/Q)$ compared to the decrease in resonance frequency, and suggests that the slip at the boundary between the atomic layers takes place in addition to that at the boundary between the film and substrate. We then applied the multilayer model above the second layer promotion, and used the following procedure to calculate the slip time for the two- and three-atom thick films:

(a) At 12.0 atoms/nm^2, which is the areal density of the second atomic layer promotion, we treat the film as a monolayer film and use Eqs. (1) and (2). Then, we obtain the slip time τ and the areal mass density σ, and determine the experimental mass loading.

(b) In the two-atom thick film, we calculate the slip times, τ_1 and τ_2, using the bilayer model by employing the areal mass density of each atomic layer from the above-mentioned mass loading and the well-known layer structure.[15,16]

(c) In the three-atom thick film, we calculate the slip times, τ_2 and τ_3, using the trilayer model under the condition that τ_1 is given.

At 12.0 atoms/nm^2, it was found that the experimental mass loading depends weakly on temperature, and becomes small at high temperature: 3.76 Hz/atoms nm^2 at 0.45 K, 3.59 Hz/atoms nm^2 at 1.0 K, and 3.48 Hz/atoms nm^2 at 1.25 K. At the moment, the temperature dependence is still an open question, and the experimental values are slightly smaller than the estimated value of 4.2 Hz/atoms nm^2.[20] However, in comparing the experimental and estimated values, it is concluded that most of the film slides uniformly relative to the oscillating substrate around the second layer promotion. Thus, since the structure of the first atomic layer does not change drastically, it is expected that the two- and three-atom thick films slide uniformly, at least when the areal density of the upper atomic layer is adequately large or the temperature is high. In the following, the slip time is calculated using the experimental mass loading at each temperature.

B. Areal density dependence

Figure 5 shows the areal density dependence of the slip time of each boundary for several temperatures.[21] It was found that the entire behavior of the areal density dependence does not depend strongly on temperature.

For the two-atom thick film, τ_1 is approximately 10 ns, and decreases slightly with increasing areal density. On the other hand, τ_2 increases with increasing areal density, and has a maximum around 17 atoms/nm^2. At this density, τ_2 is 1 order of magnitude larger than τ_1. From the comparison between τ_1 and τ_2, it is concluded that the sliding friction of the boundary between the film and the substrate is large, and the second atomic layer undergoes slipping relative to the first atomic layer with a weak sliding friction.

It is interesting to compare the areal density dependence with the phase diagram of the second atomic layer, as shown in Fig. 5(d). It was found that both τ_1 and τ_2 change discontinuously at 17 atoms/nm^2 at each temperature. In addition, τ_1 decreases rapidly above 20.5 atoms/nm^2 at 1.0 and 1.25 K, and this decrease disappears at 0.45 K. These char-

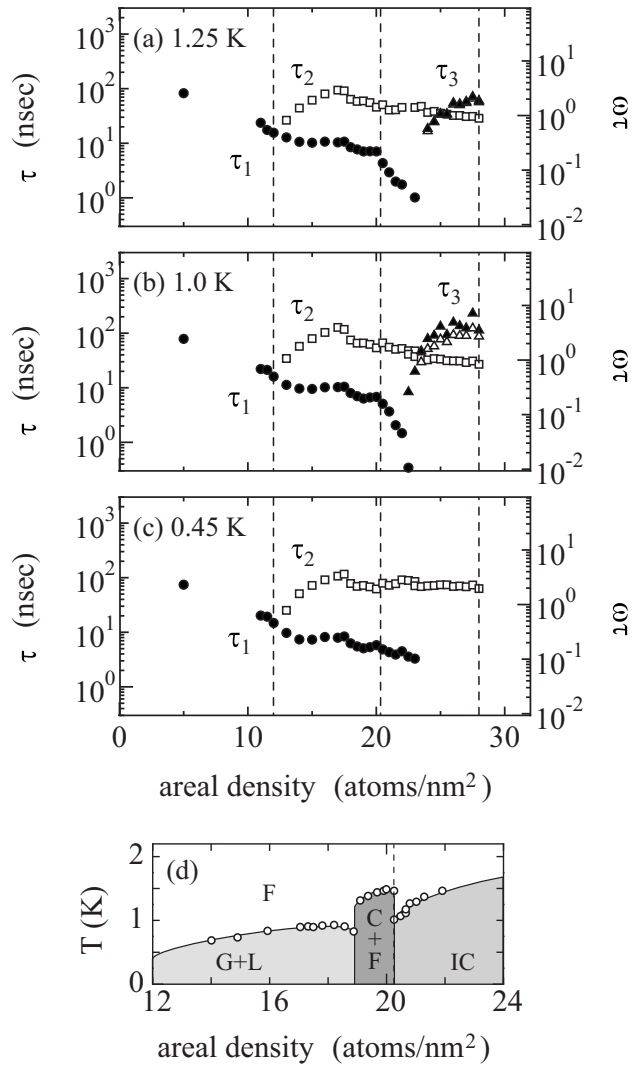

FIG. 5. Areal density dependence of the slip times at (a) 1.25 K, (b) 1.0 K, and (c) 0.45 K. Circles indicate τ_1, squares τ_2, and triangles τ_3. For τ_3, different symbols correspond to different values of τ_1 in the calculation (closed, $\omega\tau_1=0.01$; open, $\omega\tau_1=0.001$). The dotted lines indicate the layer promotions. (d) Phase diagram of the second atomic layer of ^{4}He on graphite following Crowell and Reppy (Ref. 16). Circles show the loci of heat capacity peaks from Greywall and Bush (Ref. 15). F, G+L, C+F, and IC indicate the uniform fluid phase, the gas-liquid coexistence region, the commensurate solid-fluid coexistence region, and the incommensurate solid phase. Promotion to the third layer occurs at 20.4 atoms/nm^2.

acteristic areal densities correspond to the phase boundaries, thus demonstrating that the structure of the second atomic layer has an effect on the sliding friction.

For the three-atom thick film above 22.5 atoms/nm^2, we assume that τ_1 is fixed to the extrapolated value from the two-atom thick film at each temperature.[21] Here, we adopt $\omega\tau_1=0.01$ and 0.001 at 1.0 and 1.25 K. It was found that τ_2 shows no significant difference by the choice of $\omega\tau_1$, and lies on the extrapolated curve from the two-atom thick film. On the other hand, τ_3 depends only weakly on this choice. At 0.45 K, we adopt $\omega\tau_1=0.1$. Although τ_2 does not depend strongly on this value, τ_3 is sensitive. [In Fig. 5(c), we do not plot τ_3.] We conclude that regardless of temperature, τ_2 remains large in the same manner as the two-atom thick film, and that τ_3 is also large above 1.0 K at high density.

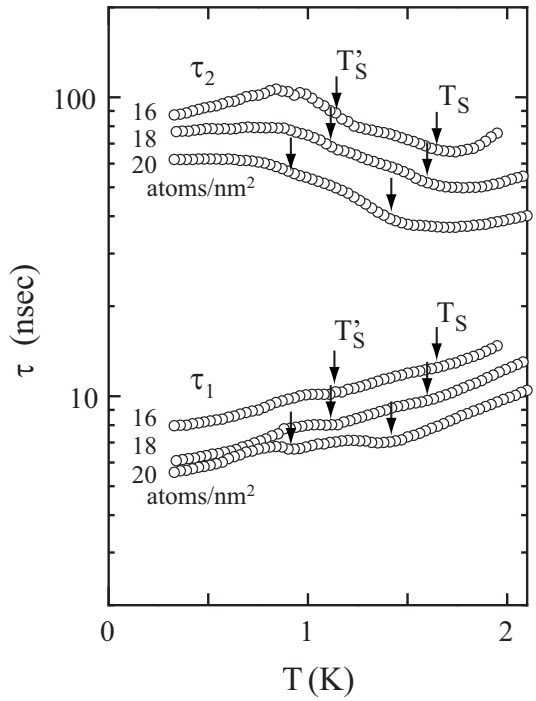

FIG. 6. Temperature dependence of τ_1 and τ_2 for several areal densities of the two-atom thick film.

Lastly in this subsection, we comment on the boundary condition of flow past the surface of Grafoil. Although there exists no direct evidence, the multilayer model may be applied to the surface in contact with liquid. Ramesh and Maynard measured solid adsorption isotherms on Grafoil in liquid ^{4}He. They found that there exists solid film on Grafoil and it grows in layers with increasing pressure.[22] Thus, we expect that the solid film in liquid ^{4}He is much the same as the adsorbed film in our experiments. For the multilayer model, we define the *effective* viscosity as $\eta_{\rm eff}=(\sigma/\tau)\cdot a$, since the sliding velocity is converted to the effective velocity gradient as v/a, where a is the thickness of one atomic layer. If we adopt $\tau_2=29$ ns and $\sigma_2=5.6\times10^{-8}$ kg/m^2 from a three-atom thick film of 28 atoms/nm^2 at 1.25 K ($a=0.36$ nm from ^{4}He atom), then $\eta_{\rm eff}=7.0\times10^{-10}$ Pa s. This value is much smaller than the normal fluid viscosity [$\eta_n=1.61\times10^{-6}$ Pa s at 1.25 K (Ref. 23)]. From the above discussion, in the case of a shear flow adjacent to the surface, the no-slip condition does not hold and the flow slips at the surface.[24]

C. Temperature dependence

Figure 6 shows the temperature dependence of the slip time for several areal densities of the two-atom thick film. It was found that τ_1 and τ_2 show different temperature dependences. τ_1 decreases gradually with decreasing temperature, and shows a weak structure. τ_2 also decreases slightly down to T_S; however, it increases below this temperature. Thus, we

can conclude that the increase in the resonance frequency below T_S, as shown in Fig. 3(b), is mainly attributable to the slip of the boundary between the first and the second atomic layers.

Next, we compare this dependence with the phase diagram of the second atomic layer, as shown in Fig. 5(d). For 16.0 atoms/nm^2, the phase boundary between F and G+L does not coincide with T_S; rather it corresponds to the temperature when τ_2 shows a maximum value. On the other hand, for 18.0 and 20.0 atoms/nm^2 the phase boundary between F and C+F is close to T_S. It is found, however, that τ_2 changes gradually around the phase boundary.

VI. SUMMARY

We have carried out a QCM experiment for multilayer ^{4}He films adsorbed on graphite. Because ^{4}He film is composed of a well-defined multilayer structure at low temperatures, we analyzed the changes of the resonance frequency and Q value using the multilayer model, and obtained the sliding friction of each atomic boundary. It was found that the sliding friction of the boundary between the first and second atomic layers is much smaller than that of the boundary between the film and the substrate.

APPENDIX A

In the multilayer model, the sliding friction acting on the substrate can be summarized as

$$F_{\mathrm{sub}} = -\frac{\sigma_1}{\tau_1}\frac{\beta + j\omega\tau}{1+\beta+j\omega\tau}\exp(j\omega t). \tag{A1}$$

Here, τ is the compound slip time and β is a constant. As an example, in the trilayer film, τ and β can be written as

$$\tau = \tau_1 + \frac{\sigma_2\tau_1}{\sigma_1\tau_2}\frac{\tau_2 + \dfrac{\sigma_3\tau_2}{\sigma_2\tau_3}\dfrac{\tau_3}{1+(\omega\tau_3)^2}}{D}, \tag{A2}$$

$$\beta = \frac{\sigma_2\tau_1}{\sigma_1\tau_2} - \frac{\sigma_2\tau_1}{\sigma_1\tau_2}\frac{1 + \dfrac{\sigma_3\tau_2}{\sigma_2\tau_3}\dfrac{(\omega\tau_3)^2}{1+(\omega\tau_3)^2}}{D}, \tag{A3}$$

where

$$D = \left\{1 + \frac{\sigma_3\tau_2}{\sigma_2\tau_3}\frac{(\omega\tau_3)^2}{1+(\omega\tau_3)^2}\right\}^2 + \left\{\omega\tau_2 + \frac{\sigma_3\tau_2}{\sigma_2\tau_3}\frac{\omega\tau_3}{1+(\omega\tau_3)^2}\right\}^2. \tag{A4}$$

APPENDIX B

We consider the resonance of the thickness-shear oscillation of a $Y(AT)$-cut quartz crystal under an oscillating shearing stress acting upon its surfaces. As shown in Fig. 7, we take the x_2 axis as the thickness direction and apply plating to the surfaces normal to this axis. Here, we take the x_1 axis as the direction of deformation.

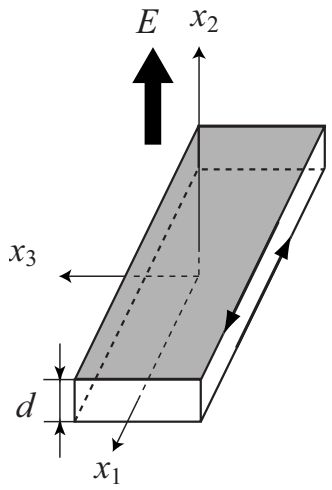

FIG. 7. $Y(AT)$-cut crystal.

Since the sectional area normal to the x_2 axis is constant, the current density $i_2 = \partial D_2/\partial t$ does not vary with the x_2 direction and

$$\frac{\partial D_2}{\partial x_2} = 0. \tag{B1}$$

For sides normal to the thickness, the stresses on the surface are zero,

$$S_4 = S_5 = 0. \tag{B2}$$

The relations between the shearing stress T_6, the electric displacement D_2, the strain S_6, and the electric field E_2 can be written in the form

$$T_6 = c_{66}^E S_6 - e_{26}E_2, \tag{B3}$$

$$D_2 = \varepsilon_{22}^S E_2 + e_{26}S_6, \tag{B4}$$

where c_{66} is the elastic stiffness, ε_{22} is the dielectric constant, and e_{26} is the piezoelectric constant. Superscript E indicates that the electric field is held constant, while superscript S that the strains are held constant. By eliminating E_2 from the first equation, we obtain

$$T_6 = c_{66}^D S_6 - e_{26}D_2, \tag{B5}$$

where $c_{66}^D = c_{66}^E\,(1 + e_{26}^2/c_{66}^E\varepsilon_{22}^S)$.

When $x_2 = d/2$ and $-d/2$ are the surfaces, the applied voltage between the electrodes is given by

$$v = \int_{-d/2}^{d/2} E_2\,dx_2 = \int_{-d/2}^{d/2}\frac{1}{\varepsilon_{22}^S}D_2\,dx_2 - \int_{-d/2}^{d/2}\frac{e_{26}}{\varepsilon_{22}^S}S_6\,dx_2. \tag{B6}$$

Under the condition of oscillating shearing stresses acting upon both surfaces, $T_6\left(\frac{d}{2},t\right)$ and $T_6\left(-\frac{d}{2},t\right)$, the boundary conditions of the surfaces can be written from Eq. (B5) as

$$\frac{\partial u_1}{\partial x_2}\left(\frac{d}{2},t\right) = \frac{1}{c_{66}^D}T_6\left(\frac{d}{2},t\right) + \frac{e_{26}}{c_{66}^D\varepsilon_{22}^S}D_2\left(\frac{d}{2},t\right), \tag{B7}$$

$$\frac{\partial u_1}{\partial x_2}\left(-\frac{d}{2},t\right)=\frac{1}{c_{66}^D}T_6\left(-\frac{d}{2},t\right)+\frac{e_{26}}{c_{66}^D\varepsilon_{22}^S}D_2\left(-\frac{d}{2},t\right), \quad \text{(B8)}$$

where the deformation of the crystal is expressed by $u_1(x_2,t)$ and $S_6=\partial u_1/\partial x_2$. Because of the symmetry against the x_2 direction, we can write the deformation with time as

$$u_1(x_2,t)=u_{1,0}\sin\left(\frac{\omega}{v_q}x_2\right)\exp(j\omega t), \quad \text{(B9)}$$

where

$$u_{1,0}=\frac{\left(\frac{T_{6,0}}{c_{66}^D}+\frac{e_{26}D_{2,0}}{c_{66}^D\varepsilon_{22}^S}\right)}{\frac{\omega}{v_q}\cos\left(\frac{\omega d}{2v_q}\right)}. \quad \text{(B10)}$$

Here, v_q is the sound velocity of the crystal, which is related to the stiffness c_{66} and the density ρ as $v_q=\sqrt{c_{66}^D/\rho}$. Subscript 0 in $u_{1,0}$ indicates the amplitude of the deformation at *the surface* of $x_2=d/2$. In the following equations, we use subscript 0 as the amplitude of the corresponding quantity at the surface.

By substituting $S_6=\partial u_1/\partial x_2$ with Eq. (B9) into Eq. (B6) and integrating the equation, the applied voltage is expressed by

$$\begin{aligned}v(t)&=\frac{d}{\varepsilon_{22}^S}D_2-\frac{e_{26}}{\varepsilon_{22}^S}\left\{u_1\left(\frac{d}{2},t\right)-u_1\left(-\frac{d}{2},t\right)\right\}\\&=\frac{d}{\varepsilon_{22}^S}\left\{1-\left(k_{26}^2+\frac{e_{26}}{c_{66}^D}\frac{T_{6,0}}{D_{2,0}}\right)\frac{\tan\beta}{\beta}\right\}D_{2,0}\exp(j\omega t),\end{aligned} \quad \text{(B11)}$$

where $k_{26}^2=e_{26}^2/c_{66}^D\varepsilon_{22}^S$, which is called the coupling constant, and $\beta=\omega d/2v_q$. For simplicity, we define the effective coupling constant as

$$k_{26}'^2=k_{26}^2+\frac{e_{26}}{c_{66}^D}\frac{T_{6,0}}{D_{2,0}}. \quad \text{(B12)}$$

Since the current density is given by $i_2=\partial D_2/\partial t$ and $i_{2,0}=j\omega D_{2,0}$, Eq. (B11) expresses the relation between the applied voltage and the current density. Then, the complex admittance defined by $Y=I/v$ is written in the crystal as

$$Y=Y_0+Y_P, \quad \text{(B13)}$$

where

$$Y_0=j\omega C_0, \quad \text{(B14)}$$

$$Y_P=j\omega C_0\frac{k_{26}'^2\frac{\tan\beta}{\beta}}{1-k_{26}'^2\frac{\tan\beta}{\beta}}. \quad \text{(B15)}$$

Here, $C_0=(\varepsilon_{22}^S/d)S$ is the capacitance, where S is the area of the electrode. Corresponding to the division of the admittance, we define the divided current $i_{2P}S=Y_Pv$. By comparison of i_{2P} with Eq. (B9), we found that this current density is directly related to the velocity at the surface, $v_1\left(\frac{d}{2},t\right)=\partial u_1\left(\frac{d}{2},t\right)/\partial t$, as

$$i_{2P}=\frac{2e_{26}}{d}v_1\left(\frac{d}{2},t\right). \quad \text{(B16)}$$

At the resonance, i_{2P} becomes maximal, and the denominator of Eq. (B15) becomes zero,

$$1-k_{26}'^2\frac{\tan\beta}{\beta}=0. \quad \text{(B17)}$$

Since $k_{26}'^2$ is small, the fundamental resonance f_R is obtained as

$$f_R=\left(1-\frac{4}{\pi^2}k_{26}'^2\right)\frac{v_q}{2d}. \quad \text{(B18)}$$

Next, we consider the change of the resonance from the condition under no stresses on the surfaces to the condition under the oscillating shearing stress acting upon its surfaces. With reference to Eq. (B18), we obtain the change Δf_R as

$$\Delta f_R=-\frac{4}{\pi^2}(k_{26}'^2-k_{26}^2)\frac{v_q}{2d}=-\frac{2v_q}{\pi^2 d}\frac{e_{26}}{c_{66}^D}\frac{T_{6,0}}{D_{2,0}}. \quad \text{(B19)}$$

At the resonance, i_{2P} becomes large and $i_{2,0}\sim i_{2P,0}$. Then, using Eq. (B16), the electric displacement $D_{2,0}=i_{2,0}/j\omega_R$ is related to the velocity at the surface as

$$D_{2,0}=\frac{1}{j\omega_R}\frac{2e_{26}}{d}v_{1,0}. \quad \text{(B20)}$$

By substituting Eq. (B19) into Eq. (B20) and using $v_q=\sqrt{c_{66}^D/\rho}$, the resonance is expressed by

$$\Delta f_R=-j4\pi f_R\frac{v_q^2}{c_{66}^D d}\frac{T_{6,0}}{v_{1,0}}=-j\frac{4\pi}{M}\frac{T_{6,0}}{v_{1,0}}. \quad \text{(B21)}$$

Since $k_{26}'^2$ is small, we use the relation $f_R\sim v_q/2d$ in the last modification. It is known that the real part of Eq. (B21) is related to the resonance frequency, and the imaginary part is the Q value. In this calculation, the oscillating shearing stresses act upon both surfaces. When the stress acts only on one side, we obtain the changes of the resonance frequency and the Q value as

$$\frac{\Delta f_R}{f_R}=-\frac{1}{\omega_R M}\mathrm{Re}\left(\frac{jT_{6,0}}{v_{1,0}}\right), \quad \text{(B22)}$$

$$\Delta\left(\frac{1}{Q}\right)=-\frac{2}{\omega_R M}\mathrm{Im}\left(\frac{jT_{6,0}}{v_{1,0}}\right). \quad \text{(B23)}$$

They are related to the ratio between the amplitudes of the shearing stress and the velocity at the surface.

*suzuki@phys.uec.ac.jp

[1] B. N. J. Persson, *Sliding Friction* (Springer, Berlin, 1998).
[2] J. Krim, D. H. Solina, and R. Chiarello, Phys. Rev. Lett. **66**, 181 (1991); C. Daly and J. Krim, *ibid.* **76**, 803 (1996).
[3] M. Highland and J. Krim, Phys. Rev. Lett. **96**, 226107 (2006).
[4] L. Bruschi, A. Carlin, and G. Mistura, Phys. Rev. Lett. **88**, 046105 (2002); A. Carlin, L. Bruschi, M. Ferrari, and G. Mistura, Phys. Rev. B **68**, 045420 (2003).
[5] L. Bruschi, G. Fois, A. Pontarollo, G. Mistura, B. Torre, F. B. de Mongeot, C. Boragno, R. Buzio, and U. Valbusa, Phys. Rev. Lett. **96**, 216101 (2006).
[6] R. Pit, H. Hervet, and L. Léger, Phys. Rev. Lett. **85**, 980 (2000).
[7] V. S. J. Craig, C. Neto, and D. R. M. Williams, Phys. Rev. Lett. **87**, 054504 (2001).
[8] A. Casey, J. Parpia, R. Schanen, B. Cowan, and J. Saunders, Phys. Rev. Lett. **92**, 255301 (2004).
[9] J. Krim and A. Widom, Phys. Rev. B **38**, 12184 (1988).
[10] L. Bruschi and G. Mistura, Phys. Rev. B **63**, 235411 (2001).
[11] N. Hosomi, A. Tanabe, M. Suzuki, and M. Hieda, Phys. Rev. B **75**, 064513 (2007).
[12] We determined the specific surface area of Grafoil through the measurement of a Kr adsorption isotherm at 77 K. After bonding Ag-plated Grafoil, the resonance frequency decreases by 0.0450 MHz from 4.9987 MHz of the bare Ag electrode at room temperature. Then, the areal density of Grafoil is calculated to be 3.64 g/m^2, and its surface area on each electrode is 56 times larger than that of the bare Ag electrode. From the molecular weight of ^{4}He, we obtained the sensitivity for the mass loading.
[13] M. J. Lea, P. Fozooni, and P. W. Retz, J. Low Temp. Phys. **54**, 303 (1984); M. J. Lea, P. Fozooni, and P. W. Retz, *ibid.* **66**, 325 (1987).
[14] In a case in which the sliding friction is not proportional to the sliding velocity, our discussion as described later is slightly modified. However, the relation between the changes in resonance frequency and Q value almost holds when we introduce the *effective* slip time τ_{eff} which depends on the oscillation amplitude of the crystal.
[15] D. S. Greywall and P. A. Busch, Phys. Rev. Lett. **67**, 3535 (1991); D. S. Greywall, Phys. Rev. B **47**, 309 (1993).
[16] P. A. Crowell and J. D. Reppy, Phys. Rev. B **53**, 2701 (1996).
[17] P. Mohandas, C. P. Lusher, V. A. Mikheev, B. Cowan, and J. Saunders, J. Low Temp. Phys. **101**, 481 (1995).
[18] M. Hieda, T. Nishino, M. Suzuki, N. Wada, and K. Torii, Phys. Rev. Lett. **85**, 5142 (2000).
[19] For a two-atom thick film of 19.5 atoms/nm^2 at 1 K, we obtain $\sigma' = 0.91 \times 10^{-5}$ kg/m^2 from Eqs. (1) and (2), while $\sigma' = 1.45 \times 10^{-5}$ kg/m^2 from the surface area of Grafoil (Ref. 12).
[20] As to the effect of desorption, the experimental mass loading is expected to decrease rapidly with increasing temperature. It was found, however, that it has a weak temperature dependence at high temperature. In addition, Grafoil disks were put on the bottom of the sample cell, and we believe that the effect of desorption was minimal for the temperature dependence under our experimental conditions. This behavior may suggest that although most of the film slides uniformly, a small portion of ^{4}He atoms, e.g., those on the edge of microcrystal, those promoted to the second atomic layer, and so on, does not slide uniformly. Then, the mass loading may increase weakly with increasing temperature.
[21] We applied the bilayer model up to 22 atoms/nm^2, although the promotion to the third atomic layer occurs at 20.4 atoms/nm^2 (Refs. 15 and 16). This means that between 20.4 and 22 atoms/nm^2, we assume that the third atomic layer moves in concert with the second atomic one. It was found that this assumption does not affect the calculated value of τ_1 because the areal density of the third atomic layer is small enough.
[22] S. Ramesh and J. D. Maynard, Phys. Rev. Lett. **49**, 47 (1982).
[23] J. T. Tough, W. D. McCormick, and J. G. Dash, Phys. Rev. **132**, 2373 (1963).
[24] By the application of the multilayer model to the surface of Grafoil in liquid ^{4}He, the slip length is expressed as $\xi = \eta_n \Sigma(\tau_i/\sigma_i)$, where η_n is the normal fluid viscosity. It is not clear how many atomic layers we should take for the surface in contact with liquid. However, if we adopt $\tau_1 \sim 0$ ns, $\tau_2 = 29$ ns, and $\tau_3 = 60$ ns from a three-atom thick film of 28 atoms/nm^2 at 1.25 K, ξ is obtained as 2.8 μm. Here, we use $\eta_n = 1.61 \times 10^{-6}$ Pa s at 1.25 K (Ref. 22).